Cellulose Nanowhisker-incorporated Poly(Lactic Acid) Composites for High Thermal Stability

Se Youn Cho, Hyun Ho Park, Young Soo Yun, and Hyoung-Joon Jin*

Department of Polymer Science and Engineering, Inha University, Incheon 402-571, Korea
(Received August 23, 2012; Revised November 11, 2012; Accepted November 16, 2012)

Abstract: In this study, biodegradable composites were prepared using cellulose nanowhiskers and poly(lactic acid). For processing at high temperature over 200 °C, cellulose nanowhiskers were prepared by ultra-sound treatment, with the high thermal stability of natural cellulose. The nanowhiskers were confirmed using transmission electron microscopy, X-ray diffraction, and thermo-gravimetric analysis. Surface modification of the cellulose nanowhiskers was performed to increase the adhesion between hydrophilic nanofillers and hydrophobic polymer matrix. The dynamic mechanical thermal analysis of the composites showed better reinforcing effect of the modified cellulose nanocrystals. The effects of cellulose nanowhiskers on the biodegradability of poly(lactic acid) were studied using a microbial oxidative degradation analyzer.

Keywords: Cellulose nanocrystals, Poly(lactic acid), Composites

Introduction

For the last century, plastics have significantly contributed to the development of industry and convenience in human life. However, the use of petroleum-based synthetic plastics has caused serious environmental problems related to solid waste, leachates, and endocrine disruptors. There has been great interest in the development of biopolymers for replacing petroleum-based synthetic plastics. However, biopolymers from renewable resources still need improved performance and cost for competition with petroleum-based polymers. To solve these problems, the use of nano-sized reinforcement has been suggested [1].

Rod-like cellulose nanowhiskers (CNWs) have attracted considerable attention as reinforcements in composite materials, on account of their exceptionally high specific strength and modulus, low density, chemical tunability, renewable nature, and relatively low cost [2-6]. However, the industrial use of CNWs is still limited due to the difficulty of dispersing them in polymer matrix, and their low thermal stability [7,8]. The large number of hydroxyl groups of cellulose and the nonpolar characteristics of most thermoplastics result in difficulties in achieving acceptable dispersion levels of nanofiller in the matrix, which results in inefficient composites with weak interfacial bonding. Moreover, the common method to prepare CNWs from native semicrystalline cellulose is to use sulfuric acid hydrolysis to break the substance down into its elementary crystalline domains by removing amorphous cellulose segments [2,7], which results in the introduction of sulfate groups on the surface of CNWs by esterification during hydrolysis, as well as a rapid diminishing in its degree of polymerization [8,9]. Consequently, a considerable decrease in degradation temperatures has been observed compared to native cellulose, and this reduction of thermal stability interrupts

their use in composites with thermoplastics typically processed at temperatures over 200 °C [7,8].

In this study, we prepared CNWs with high thermal stability by a simple sonication method. We also prepared poly(lactic acid) (PLA)/CNW composites to study the reinforcing effects of CNWs on the thermal and mechanical properties of PLA.

Experimental

Materials

PLA with an average molecular weight of 200,000 g/mol (2002D-Grade) manufactured by Natureworks Co. (USA) was used. Microcrystalline cellulose (MCC) powder and all of the reagents, acetic acid, dry toluene, 70 % perchloric acid, and acetic anhydride, were purchased from Sigma-Aldrich.

Preparation of CNWs

10 g of MCC powder were added to 200 m*l* of DI water. After sonication for 24 hours using an ultrasonic generator (Kyungill Ultrasonic Co., Korea), 1 *l* of DI water was added and allowed to stand for 24 hours. The supernatant of the suspension was separated and centrifuged for 20 min at 5000 rpm. For comparison, S-CNWs were prepared (cellulose nanowhiskers prepared by typical sulfuric acid hydrolysis). 10 g of MCC powder were added to 65 wt% sulfuric acid with an acid-to-cellulose ratio of 1:8.75 (g/m*l*). The solution was stirred continuously at 45 °C for 1 h. The resulting S-CNWs were collected and purified by repeated centrifugation (9500 rpm, 30 min) and dialysis for 7 days. Both types of CNWs were re-dispersed in DI water and subject to sonication for one hour in ambient conditions.

Surface Acetylation of CNWs

The surface modification of CNWs was conducted by a

---

*Corresponding author: hjjin@inha.ac.kr

route reported elsewhere [10]. The solvent of the CNWs in aqueous suspension (100 mg/ml) was exchanged with acetone and then dry toluene. CNWs ware placed in a 500-ml beaker containing a mixture of 108 g of toluene, 105 g of acetic acid, and 0.5 ml of 70 % perchloric acid. After vigorous stirring for 1 min, 54 g of acetic anhydride were added, and the mixture was stirred vigorously for 1 min. The mixture stood for 1 h at room temperature. After the reaction of CNWs, the modified CNWs were washed thoroughly 3 times with methanol, then 3 times with DI water.

PLA/CNWs Composites Film

PLA/CNW composite films were prepared using a solvent mixture, followed by hot pressing. The solvents of the CNWs and A-CNWs in aqueous medium were exchanged to acetone and then to chloroform, with centrifugation and re-dispersion steps. To measure the concentration of CNWs, a small amount of CNWs in chloroform was cast in a glass dish and allowed to evaporate. PLA pallets were gradually added while stirring the CNWs suspended in chloroform. After sufficient stirring, the mixture was cast and allowed to evaporate with vacuum-oven drying at 55 °C for 5 days. After crushing into small pieces, the composite films were obtained by hot pressing at 200 °C.

Characterization

To confirm the morphology of CNWs, transmission electron microscopy was used (TEM, CM200, Philips, Netherlands). The thermal stability of CNWs was determined using a thermo-gravimetric analyzer (TGA, TA Instruments Q50, U.K.). Fourier transform infrared spectroscopy (FT-IR, VERTEX 80v, Bruker Optics, Germany) was used for studying the structures of the modified CNWs. Dynamic mechanical measurements (DMA, Q800, TA instruments, U.K.) and differential scanning calorimetry (DSC, Perkin Elme Jade) were used to study the thermal and mechanical properties of PLA/CNW composites. A biodegradation test was employed to investigate the biodegradability of PLA and its composites using a Microbial Oxidative Degradation Analyzer (MODA).

Results and Discussion

Preparation of CNWs

The preparation scheme for CNWs by simple sonication method is illustrated in Figure 1. A long ultra-sonication time could allow for the creation of fragments from MCC. Among the shreds, small fragments disperse and float in water. We acquired these floating materials and investigated their characteristics. TEM images were used to confirm the morphology of the CNWs produced by sonication. As shown in Figure 2(b), more aggregates and broader boundaries could be found compared with the S-CNWs (Figure 2(a)). However, it was clearly confirmed that the CNWs were
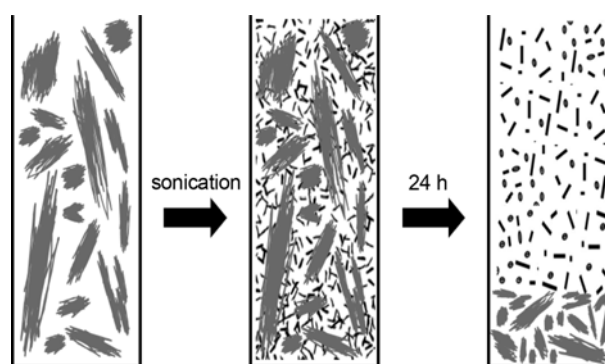
**Figure 1.** Schematic illustration for the CNW preparation by sonication.
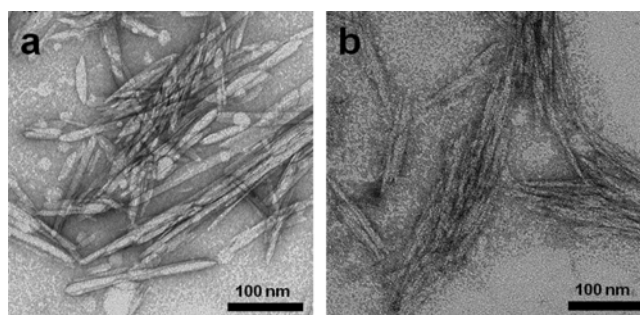
Figure 2. TEM images of the CNWs prepared by sulfuric acid (a) and sonication (b).
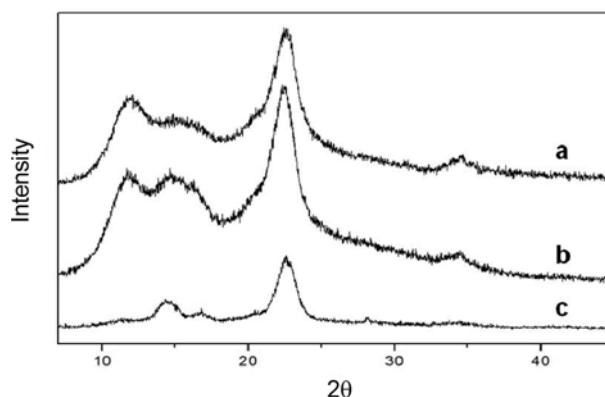
Figure 3. WAXD pattern of CNWs by sulfuric acid (a) and sonication (b), and microcrystalline cellulose (c).

formed with long length and width less than 10 nm. The individual existence of the S-CNWs is due to the electrostatic repulsion between the surface negative charges of the sulfate group introduced during acid hydrolysis [6]. In addition, ultra-sound generated less break-down of the amorphous region compared with acid treatment, which resulted in the appearance of broader boundaries of the CNWs by sonication.

Figure 3 shows the XRD patterns of MCC, CNWs prepared by sonication, and S-CNWs. In the patterns of the
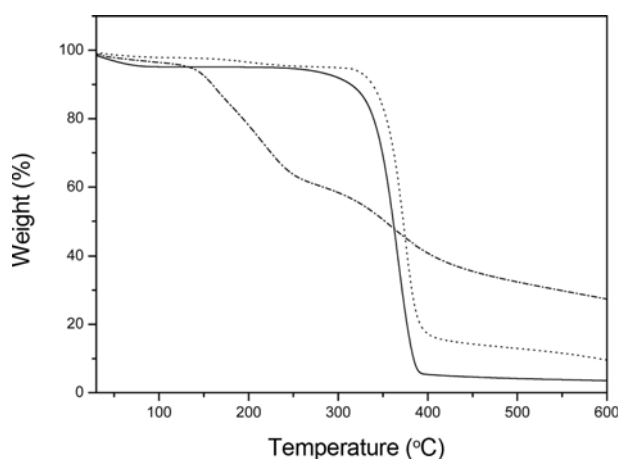
Figure 4. TGA curves of CNWs prepared by sulfuric acid (dashed line) and sonication (dotted line), and microcrystalline cellulose (solid line).


Figure 5. FTIR spectra of (a) CNWs and (b) modified CNWs obtained by sonication. The optical image shows the dispersion of CNWs and modified CNWs in chloroform.

CNWs prepared by sonication, additional peaks can be seen at $2\theta=14.5\,^{\circ}$ and $16.4\,^{\circ}$, whereas a broad shoulder around the region of $2\theta=14\,^{\circ}$ to $17\,^{\circ}$ can be seen in the case of MCC [13]. With the higher intensity of the diffraction peak at $2\theta=22.5\,^{\circ}$, the peaks that are more prominent and sharp for the CMWs by sonication indicate an increase in crystallinity, which confirmed that the break-down of an amorphous region of the MCC existed during the ultra-sound treatment. Meanwhile, the S-CNWs present distinct diffraction peaks centered at $2\theta=14.5\,^{\circ}$, $16.4\,^{\circ}$, and $22.5\,^{\circ}$, corresponding to a typical form of cellulose I, showing high crystallinity as a result of strong chemical hydrolysis of the amorphous region.

The thermal-degradation curves were measured, and are plotted in Figure 4. The thermal analysis showed that the thermal degradation of S-CNWs (Figure 4, dotted line) was initiated at a lower temperature (125 ^{o}C). The low thermal degradation resulted from the introduction of sulfated groups into S-CNWs during the sulfuric acid hydrolysis process, which could reduce the thermostability of the S-CNWs [6,7]. In contrast, the CNWs prepared by sonication (Figure 4 dash line) showed thermal degradation behavior similar to that of MCC (Figure 4, solid line), which began at over 250 ^{o}C. Also, the temperature at the onset of degradation (temperature at 5 % weight loss) of the CNWs prepared by sonication was much higher than that of the S-CNWs (approximately 300 ^{o}C and 170 ^{o}C, respectively).

Surface Acetylation of CNWs

To achieve the stable dispersion of CNWs in non-polar organic solvent, the surface acetylation of CNWs was performed. Figure 5 shows the FT-IR spectra of CNWs and acetylated CNWs. As a result of esterification, the IR spectra of the modified CNWs showed a significant decrease in the O-H band (3338 cm^{-1}) and increases in three major bands of cellulose triacetate, i.e. the C=O stretching mode (1740 cm^{-1}),
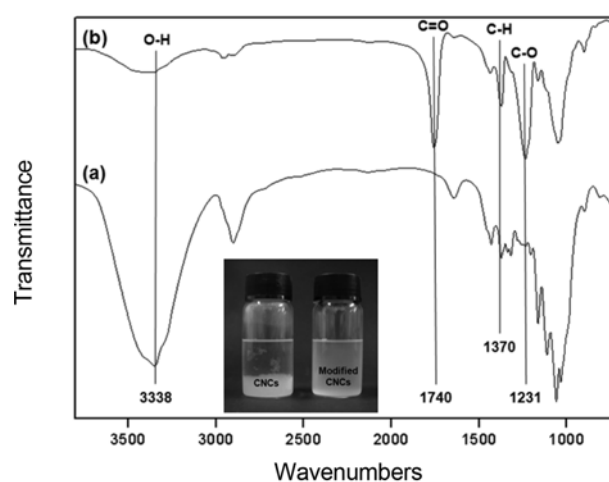
the C-O stretching mode (1231 cm^{-1}), and the C-CH$_3$ asymmetric bending vibration mode (1371 cm^{-1}) [10]. An optical image of the CNWs and acetylated CNW dispersion in chloroform shows that the surface modification of CNWs led to improvement of the dispersibility in the hydrophobic organic solvent. A number of hydrophilic hydroxyl groups were substituted with hydrophobic groups, which may induce good adhesion for the CNWs with the polymer matrix.

PLA/CNWs Composite

Visual optical images of neat PLA and PLA composite films with different types of CNWs are presented in Fig. 6. As shown in Figure 6(b), the PLA composite film with the S-CNWs includes many black spots, which are traces of the CNW pyrolysis that occurred due to low thermal stability. Some vague spots are also visible in the PLA/CNW film (Figure 6(c)), which happened because of CNW aggregation caused by poor compatibility between the CNWs and the polymer matrix. However, there were no vestiges of thermal degradation or agglomeration on the PLA composite films with modified CNWs (Figure 6(d)), which provides evidence of increased compatibility between the cellulose nano-filler and the polymer matrix as a result of the surface modification of the CNWs.

The thermograms of DSC for neat PLA, PLA/CNW composite, and PLA/acetylated CNW composite were shown in Figure 7 and summarized in Table 1. In Figure 7(a), the glass transition temperature (T_g), cold crystallization temperature (T_{cc}), and melt temperature (T_m) of neat PLA are shown on the curve of the first heating scan. During the cooling scan, the thermogram shows a very weak and broad peak of melt crystallization temperature (T_{mc}). In the second heating, the thermogram still exhibits T_g and T_{cc}, indicating incomplete crystallization during the cooling scan because of its low
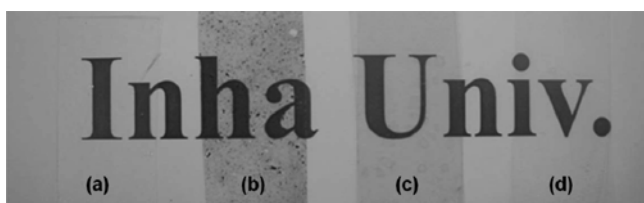
Figure 6. Photographs showing the appearance of the composite films. (a) Neat PLA, (b) PLA/CNWs prepared by acid treatment, (c) PLA/CNWs prepared by sonication, and (d) PLA/modified CNWs prepared by sonication.

Table 1. DSC Data of neat PLA and the PLA/CNWs nanocomposites

	T_g (^oC)	T_{cc} (^oC) (1st heat)	T_{mc} (^oC)	Crystallinity (%)* (after cooling)
Neat PLA	61.1	103.2	-	24.7
PLA/CNWs	61.4	102.3	100.1	44.9
PLA/acetylated CNWs	62.4	100.2	101.7	53.4

*The theoretical melting enthalpy of 100 % crystalline PLLA was taken (DH1m=93.0 J/g) [14].

crystallization rate. The thermogram of the PLA/CNW composite (Figure 7(b)) shows different behavior compared to the thermogram of neat PLA. The PLA/CNW composite appears to have lower T_{cc} (102.3 ^oC) and higher T_{mc} (101.7 ^oC). It shows that the PLA/CNW composite started to crystallize faster than neat PLA, which indicates that the CNWs can act as a nucleating agent for the crystallization of PLA. In the second heating, the thermograms of the PLA/CNW composite exhibits only T_{mc}, while T_g and T_{cc} are almost absent, indicating that the material was highly crystalline after the cooling scan. The thermogram of PLA/modified CNWs shows lower T_{cc} and higher T_{mc} than those of the PLA/CNW composite. It seems that the modification of CNWs could

allow them to disperse evenly in the polymer matrix and offer more nucleation sites for the crystallization of PLA.

DMA analysis provides information the mechanical properties and molecular relaxations that occur in the polymer composites during heating. Figure 8 shows the storage modulus and tan delta as functions of temperature. In Figure 8(a), neat PLA showed constant storage modulus in the glassy region. With increase in temperature, the storage modulus decreased gradually after T_g, 60 ^oC. The decrease of modulus around T_g is due to α-relaxation of amorphous structure [12]. PLA/CNW composites revealed slightly improved storage modulus compare with neat PLA in glassy region, whereas at 70 ^oC the modulus increased dramatically. Such a high storage modulus at high temperature supported
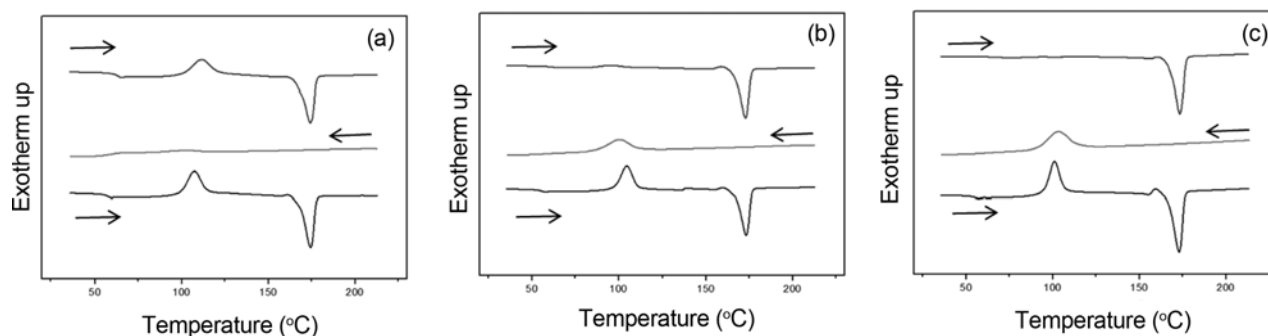
Figure 7. DSC curves of (a) neat PLA and PLA composite reinforced with (b) unmodified CNWs, and (c) modified CNWs obtained by sonication method.
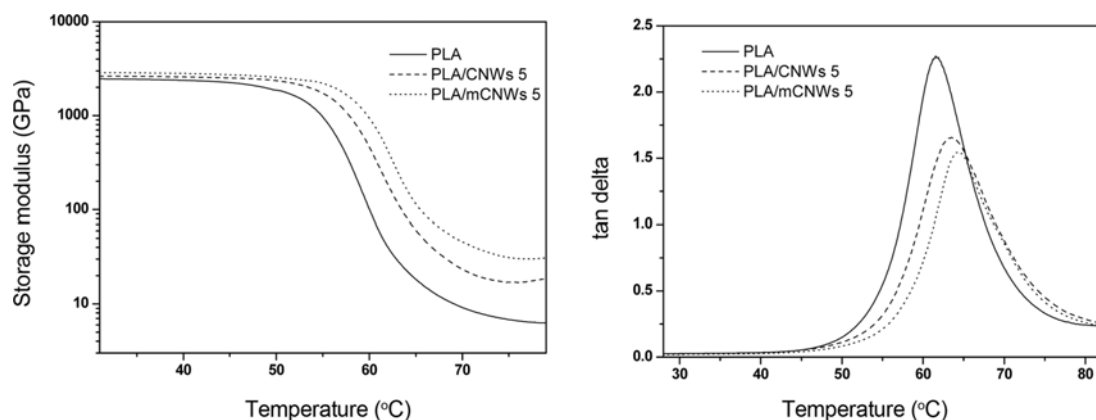
Figure 8. DMA analysis of neat PLA and PLA composites; storage modulus (left) and tan delta (right) curves.
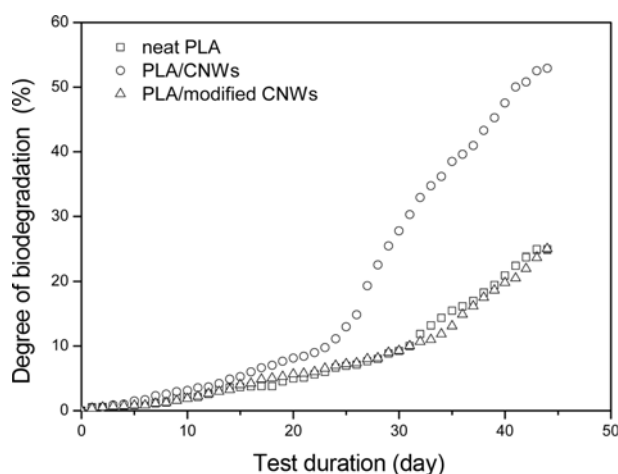
Figure 9. Biodegradabilities of PLA and its composites in controlled compost at 58 °C by MODA.

the reinforcing effect and crystallization of PLA by addition of nanofillers. In Figure 8(b), the tan delta peak is shifted to a higher temperature, and has decreased intensity after the addition of CNWs. The decreased intensity indicates that fewer polymer chains are participating in this transition, due to the high crystallization resulting from the addition of nanofillers. The shift demonstrates that nano-sized CNWs interrupt the segmental mobility of the polymer chains. A greater increase in the storage modulus and a positive shift in the tan delta peak position were shown in the PLA/modified CNW composites, which can be attributed to the high level of interaction between the polymer and reinforcements by surface modification.

Biodegradability

The behavior of the degradation of PLA and its composite were measured by a MODA instrument for 45 days. Considering the applications of biodegradable polymers, composting could be suggested as the most proper disposal route. Biodegradation test using a MODA apparatus involves the use of controlled composting under high humidity and temperature of around 58 °C. These conditions are known to provide a suitable environment for the hydrolytic degradation of polymers. The degree of biodegradation percentage was calculated from the amount of CO_2 produced. Figure 9 shows the biodegradation of neat PLA and its composites. After the induction periods of about 20-30 days, the degradation rates were accelerated. Particularly, PLA/CNWs composite showed a short induction period and much higher degradation rate compared to neat PLA and PLA/acetylated CNW composite. During the polymer degradation, moisture susceptibility is the primary driving force towards degradation, and involves four steps: water absorption, ester cleavage forming oligomers, solubilization of oligomer fractions, and diffusion of soluble oligomers by bacteria [13]. The high water absorption that brought about the hydrophilicity of

CNWs led to a short induction period and faster degradation rate of the PLA/CNWs composite. In addition, the pores formed by degradation of CNWs also accelerated water absorbance [14]. However, PLA/acetylated CNW composite shows similar behavior to neat PLA due to the decrease of the CNW hydrophilicity.

Conclusion

Acknowledgments

References

1. L. Petersson, I. Kvien, and K. Oksman, *Compos. Sci. Technol.*, **67**, 2535 (2007).
2. Y. Habibi, L. A. Lucia, and O. J. Rojas, *Chem. Rev.*, **110**, 3479 (2010).
3. A. C. W. Leung, S. Hrapovic, E. Lam, Y. Liu, and K. B. Male, *Small*, **7**, 302 (2011).
4. O. V. D. Berg, J. R. Capadona, and C. Weder, *Biomacromolecules*, **8**, 1353 (2007).
5. Q. Wu, M. Henriksson, X. Liu, and L. A. Berglund, *Biomacromolecules*, **8**, 3687 (2007).
6. J. R. Capadona, O. Van den Berg, L. A. Capadona, M. Schroeter, S. J. Rowan, G. J. Tyler, and C. Weder, *Nat. Nanotechnol.*, **2**, 765 (2007).
7. M. A. S. A. Samir, F. Alloin, and A. Dufresne, *Biomacromolecules,* **6**, 612 (2005).
8. M. Roman and W. T. Winter, *Biomacromolecules*, **5**, 1671 (2004).
9. H. Hakansson and P. Ahlgren, *Cellulose*, **12**, 177 (2005).
10. D.-Y. Kim, Y. Nishiyama, and S. Kuga, *Cellulose*, **9**, 361 (2002).
11. F. G. Hurtubise, *Tappi*, **45**, 460 (1962).
12. L. Suryanegara, A. N. Nakagaito, and H. Yano, *Compos. Sci. Technol.,* **69**, 1187 (2009).
13. S.-S. Wong, S. Kasapis, and Y. M. Tan, *Carbohyd. Polym.,* **77**, 280 (2009).
14. A. Pei, Q. Zhou, and L. A. Berglund, *Compos. Sci. Technol.,* **70**, 815 (2010).
15. M. Funabashi, F. Ninomiya, and M. Kunioka, *Int. J. Mol. Sci.*, **10**, 3635 (2009).
16. A. P. Mathew, K. Oksman, and M. Sain, *J. Appl. Polym. Sci.*, **97**, 2014 (2005).